

Sprayed Earth Additive Manufacturing: A Novel Manufacturing Process for Earthen Materials

Joschua Gosslar¹, Gerardo Arcangelo Pacillo², Noor Khader¹, Harald Kloft¹ and Norman Hack¹

¹Technische Universität Braunschweig, Institute of Structural Design, Braunschweig, Germany

²University of Florence, Department of Civil and Environmental Engineering, Florence, Italy

Correspondence to:

Joschua Gosslar
Technische Universität Braunschweig,
Institute of Structural Design,
Braunschweig, Germany.
E-mail: j.gosslar@tu-braunschweig.de

Received: July 25, 2023

Accepted: September 26, 2023

Published: September 28, 2023

Citation: Gosslar J, Pacillo GA, Khader N, Kloft H, Hack N. 2023. Sprayed Earth Additive Manufacturing: A Novel Manufacturing Process for Earthen Materials. *NanoWorld J* 9(S2): S238-245.

Copyright: © 2023 Gosslar et al. This is an Open Access article distributed under the terms of the Creative Commons Attribution 4.0 International License (CCBY) (<http://creativecommons.org/licenses/by/4.0/>) which permits commercial use, including reproduction, adaptation, and distribution of the article provided the original author and source are credited.

Published by United Scientific Group

Abstract

This paper describes a novel digital earthen fabrication concept referred to as Sprayed Earth Additive Manufacturing (SEAM), where earthen material is sprayed robotically with pressure in order to create a three-dimensional structure. Compared to processes based on material-extrusion, the adhesion between the sprayed layers is improved, the addition of material is controlled, and spatial flexibility is enhanced. Additionally, the possibility of adding natural fibers to the sprayed earthen mix allows enhancing the strength and the shrinkage behavior of the earthen material. The paper starts by addressing the current state of the art on reinforcement of earthen material, optimization of the spraying technique and automation in the construction process. It then demonstrates the applied methodology, early material research, explored spraying parameters such as the influence of air volume flow, nozzle velocity and nozzle to strand distance on the layer geometry and the implemented robotic fabrication setup for integrated fiber reinforced spraying. A novel concept of fiber integration, where a continuous fiber strand is chopped and added to the sprayed earthen material directly at the nozzle, was tested for the first time. Finally, the paper presents a series of the latest experimental results, reflections on the overall material reinforcement investigations and concludes with potential future explorations needed for the research.

Keywords

Sprayed earth, Additive manufacturing, Earthen materials

Introduction

Since 3D printing technologies have become more prevalent in the construction industry and the movement towards reducing environmental impact has been growing, earthen materials have undergone a significant shift in the way they are perceived as well as the way they are integrated within the construction process [1]. This development of new earthen digital manufacturing processes complements existing traditional manufacturing methods, opening up new avenues for the construction of earthen structures [2, 3]. With the demands of construction processes today characterized by short design and building periods, increased quality, and reduced costs, automation can have a tremendous impact [4]. The construction industry accounts for 11% of the global CO₂ emissions [5]. The use of both digital planning and production techniques could lead to increased efficiency of construction methods and thus, optimized use of materials [3]. Material-process combinations based on the use of fully recyclable and cement-free options with a low carbon footprint such as earthen materials could significantly reduce the carbon footprint of the construction industry. As a result of the use of computer-aided manufacturing, earthen structures can now be produced more efficiently and at a lower cost than they would otherwise be if making use of

artisanal methods. Furthermore, digital fabrication techniques allow for a greater degree of geometric freedom, thus creating the possibility of achieving advanced functional integration as well as new forms of expressive design [3].

The SEAM approach has its roots in a manual spraying process that has been refined over the past few decades, known as Pneumatically Impacted Stabilized Earth [3, 6]. In this method, a cement-clay mixture is conveyed by air pressure to the spray nozzle, where it is mixed with water as it exits; the mix is then sprayed under high pressure [6]. In a similar fashion, using the SEAM technique, unstabilized earthen material is sprayed robotically and mixed with chopped fibers after the earthen material leaves the nozzle. It is commonly practiced strengthening earthen building materials by using fibers of various types as a result of their low tensile strength, thus enhancing their durability [7]. Various earth-based construction materials, such as adobe, cob, and earth plasters, rely on plant fibers for reinforcement as a basic method of strength enhancement [8-10]. The use of plant fiber reinforced earth is not only environmentally friendly but its capability of achieving compressive and tensile strengths similar to cement or lime-stabilised earth has been demonstrated, reducing the stiffness significantly and leading to a more ductile composite material [9].

The use of earthen granular substances as main building material has been prevalent throughout history. In order to improve the durability and mechanical performance of earthen materials, a variety of natural fibers (e.g., straw), as well as manmade stabilizers (e.g., cement and lime), have been explored in different earthen construction processes. An example of one of the earliest vernacular earth construction methods is the Cob technique, which involves mixing excavated sub-soil with organic topsoil and placing it on to a wall to create a monolithic, load-bearing structure [11, 12]. This technique was generally associated with the addition of natural fibers, especially long fibers (40 - 60 cm), with a fiber length approximately equal to the width of the wall (Figure 1) [12]. In spite of the fact that cob is a constantly evolving technique [12], the modern implementations still result in solid and massive earthen structures (Figure 2).

As 3D extrusion-based technologies become more widespread, they offer new possibilities to the construction industry and change the way that architectural elements are designed and manufactured. A few 3D printed earthen projects that conclude this premise are the 3D printed clay wall by IAAC and WASP and the 3D printed clay house by Mario Cucinella Architects (Figure 3 and figure 4) [13, 14]. Both of these projects illustrate the current state of the art with respect to 3D printed earthen structures, where the extrusion technique of earthen material enables greater geometric flexibility, material optimization, and also functional integration. A noteworthy point here is that earthen mixes are still bound by the limiting incorporation of long fibers, which hinders material flow during the extrusion process due to fabrication related parameters such as the nozzle diameter.

Another additive manufacturing process called Shotcrete 3D Printing (SC3DP) has been developed at TU Braunsch-



Figure 1: Earthen wall constructed with the Cob technique.



Figure 2: The CobBauge research building at The University of Plymouth, 2020.

weig in order to overcome various fabrication limitations associated with extrusion-based 3D printing (Figure 5) [15, 16]. SC3DP offers good layer bonding, enables embedding of rebars integrated horizontally and vertically, and the ability to spray on vertical surfaces to build up material horizontally [16]. The process of spraying concrete results in an augmented interlayer contact surface area in comparison to extrusion [17], yielding a favorable impact on interlayer strength [18, 19]. Consequently, this technique holds potential benefits in terms of reducing anisotropy. In addition, the distance between the nozzle and the target position (nozzle distance) provides an opportunity to incorporate additional aggregates, fibers, or additives before forming the ultimate layer. As such, the use of SC3DP with fiber reinforced earthen mix was considered a promising area for further research and investigation (Figure 6).

Experimentation

Basic fabrication setup

The Digital Building Fabrication Laboratory (DBFL) at the Institute of Structural Design (ITE) at TU Braunschweig is the basis of the research activities at ITE. On a built space of 10.5 x 2.25 x 2.5 m, a CNC-controlled 5-axis portal milling machine and a 6-axis robot are suspended from a 3-axis gantry. The laboratory offers the possibility to fabricate large-format components, rapidly develop prototypical additive manufacturing procedures and research automated manufacturing processes, using a wide range of production techniques.

The process chain used for SEAM comprises several devices and components. The general setup consists of a mortar pump with a hose connected to a customized spray system, which is mounted to a robotic arm. The auger pump used includes the rotor stator set 2L6 with a throughput of 65 L/min at 400 rpm and a maximum grain size of 8 mm. In order to enhance fluidity of the viscous material in the pump, a concrete vibrator was used permanently during the pumping process. A mortar hose with an inner diameter of 50 mm and a total length of 10 m was used to convey the material to the spray system. The spray system consists of a hose connection and a distributor fitting in which the viscous material is accelerated by air pressure and sprayed through a conic shaped vulkollan nozzle with a nominal width of 15 mm. A digitally controlled pneumatic pinch-valve allows to precisely start and stop the spraying process. The advanced setup including the fiber cutting mechanism is described in Paragraph "Additional fiber reinforcement" below.

Material

In order to successfully build durable and qualitative elements with the SEAM technique, it is necessary to carefully consider the material properties in both the wet and hardened state. In its wet phase, the material undergoes the first process steps: mixing and pumping, transportation to end-effector and consequential deposition of layers via spraying. During these phases, material properties concerning the 3D print [20] such as printability, workability, buildability, and time-dependent behavior of the material must meet the process demands. On the one hand, that means that the material must be fluid enough to be pumped through the hose until the end-effector's chamber. Here in SEAM, unlike in the extrusion/deposition process of 3D printing, the material is combined with compressed air and propels inside the end-effector's mixing chamber, then sprayed out layer by layer. On the other hand, during the printing process, the material must be stiff enough to support several layers without causing large geometrical deformations. After hardening, the material reaches its full structural integrity, being able to perform under mechanical loads, and, finally, meeting the overall construction requirements. The earth mixtures in this study were prepared aiming to meet the requirements of both the fresh and hardened states.

The mixture's main components are clay, silt, and sands of different grain sizes (though all grains fall below the size of 1.4 mm to avoid problems with the printing system). The clay used was supplied by the company Conluto [21], which



Figure 3: 3D printed clay wall by IAAC and WASP.



Figure 4: 3D printed clay house by Mario Cucinella Architects and WASP.



Figure 5: Additive manufacturing based on spaying: SC3DP, ITE, TU Braunschweig.

has been adapted for 3D printing processes. The clay particles

were a mixture of 45% kaolinite, 45% illite, and 10% smectite (results obtained by X-ray diffraction analysis). Clay and sand were previously mixed in their dry state to ensure optimal homogenization. Subsequently, water was added to make the mixture workable. Water contents of 20, 25, and 30% were tested, giving that a water content lower than 20% does not allow the mixture to be pumpable, affecting the process and the printing quality, and a content greater than 30% compromises the rheology of the material, making it unusable for the printing and construction phase. The study concluded that in terms of pumpability, 20% water content with 52% clay and 48% sand allows for a steady/smooth flow and greater layer stability, compared to 25 and 30% moisture content. Sprayed earths are nanoscale materials.

Fabrication parameters

The process of SEAM is defined on a fundamental level by several sub-processes and the sequence in which these processes are arranged. In the present case, the following sequence was used: 1. Mixing, 2. Pumping, 3. Propelling of the material by air pressure, 4. Integration of fibers, and 5. Application to the substrate. Through the described sequence, the target material properties can be described as pumpable, sprayable, and buildable [20]. The material-process interaction in SEAM is comparable to the SC3DP process [22]. The important sub-processes' parameters influencing the overall fabrication technique are described below.

The length, inner shape, and nominal width of the spraying nozzle affect the geometry of the resulting layer and the homogeneity of the material-jet. The pump speed relates to the viscosity of the material and the specifics of the pump itself,

such as size and speed of rotation of the rotor and stator, the friction in the hose defined by the hose's inner diameter, condition, and length of surface as well as gravity, in case the material is pumped vertically. Identifying the correct pump speed allows for a continuous and homogeneous flow of material inside the hose. A pump-speed that is set too high results in excessive supply of material or excessive pressure build-up inside the hose. In contrast, a pump speed that is set too low increases fabrication time or leads to interruption of conveying in case friction within the hose exceeds pumping pressure. It is desirable to have a consistent conveying flow throughout the fabrication process.

Results and Discussion

A parameter study was conducted to compare the influences of actively controllable fabrication parameters on the resulting layer geometry, which is predominantly defined by the layer width (LW) and layer height (LH). Therefore, the influence of fabrication variables such as nozzle velocity (NV), nozzle distance (ND) and Volume Air Flow (VAF) on the layer geometry was evaluated in a test campaign at DBFL.

Nozzle velocity

The NV describes the travel speed of the end effector measured at the Tool Center Point. In the study, varying NV in a range of 2400 mm/min to 6000 mm/min and varying ND between 100 mm and 200 mm with a fixed VAF of 30 m³/h were tested. The respectively resulting LW and LH are plotted in figure 7 and figure 8. The range of resulting LW is between 145 mm and 205 mm and the range of resulting LH is between 23 mm and 44 mm. What is also recognizable is an increase of the LW and decrease of the LH while increasing the ND from 100 to 200 mm. Moreover, a 100% increase of the NV (2400 to 4800 mm/min) leads to reduction of 21% in LW (190 to 150 mm) and 34% in LH (44 to 29 mm) at a ND of 100 mm with the results being in line with the expectations regarding observations from SC3DP.

Volume air flow

Controlled addition of compressed air propels the material at the spray nozzle, resulting in a fine material jet with a

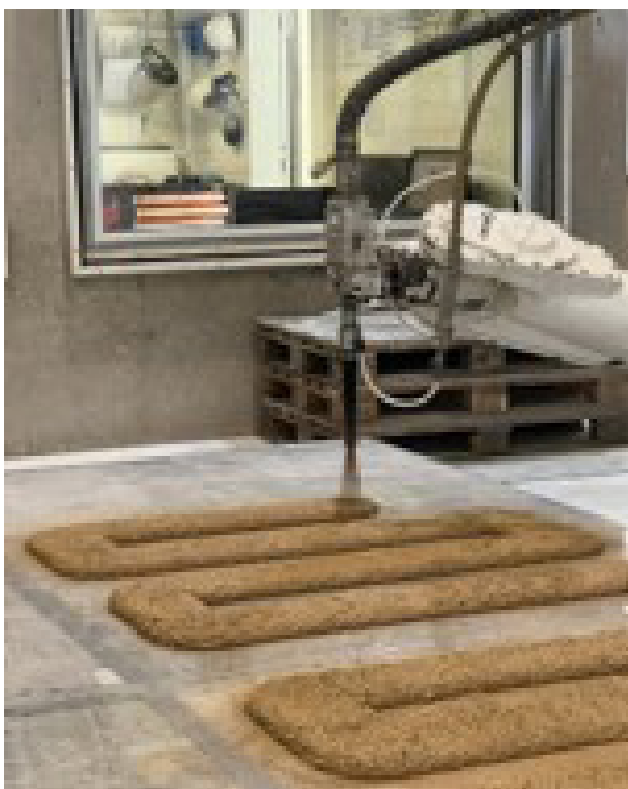


Figure 6: Additive manufacturing based on spraying: SEAM, ITE, TU Braunschweig.

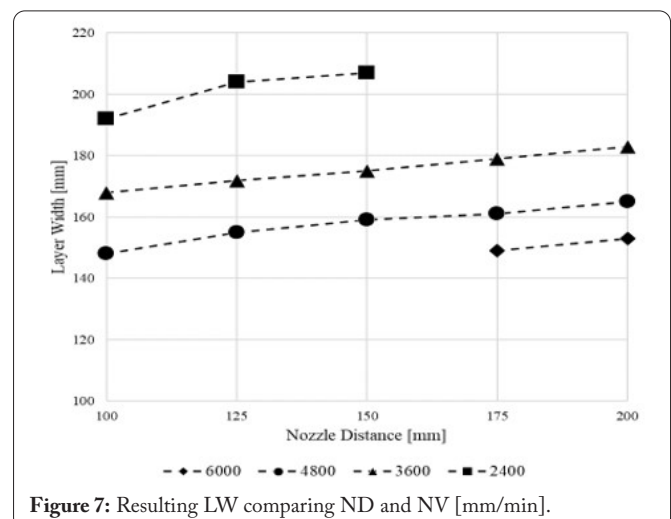


Figure 7: Resulting LW comparing ND and NV [mm/min].

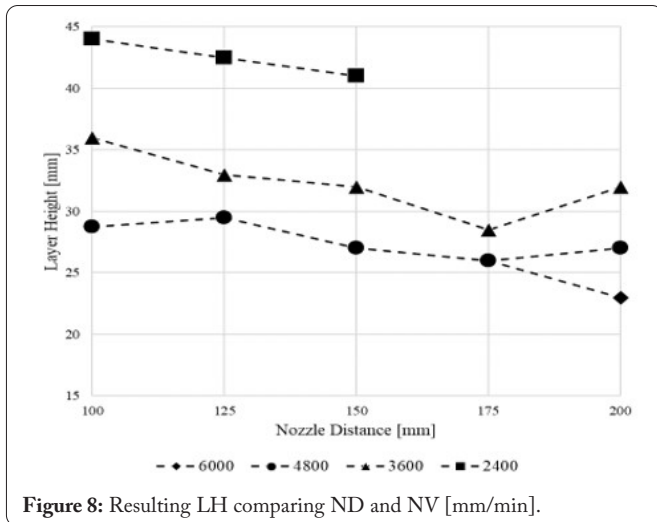


Figure 8: Resulting LH comparing ND and NV [mm/min].

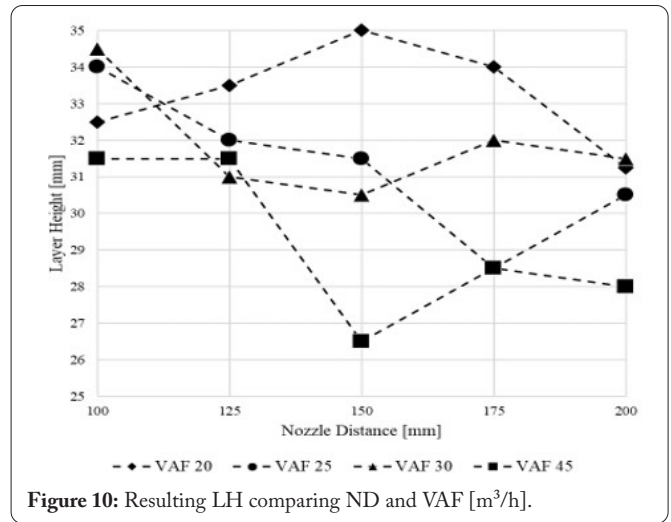


Figure 10: Resulting LH comparing ND and VAF [m³/h].

high contact surface area between air and material. The compressed air forces the material-jet through the nozzle and results in an impact with high speed on the substrate layer creating a high layer bond through compaction and adhesion. The applicable range of values for VAF is defined by the resistance of the substrate layer to the impact forces of the material jet as an upper limit and, conversely, an accumulation of material in the nozzle leading to blockage as a lower limit.

In a parameter study, the resulting LH and LW were measured at different VAFs and with different ND at a NV of 4000 mm/min (Figure 9 and figure 10). In a range of 163 - 179 mm of LW and 26.5 - 35 mm for LH, no linear trend between VAF and layer geometry is observed, which suggests that VAF is not a major factor influencing the layer geometry and is again in line with results from SC3DP attained by Dressler et al. [17].

Material moisture content

Opposed to cementitious materials, humidity in earthen materials is not bound into the matrix in a chemical curing process. Thus, humidity needs to fully evaporate in order for the material to gain ultimate strength, which leads to geometrical shrinkage and the occurrence of cracks. Increased water content reduces viscosity and improves pumpability. Hence,

controlling the humidity of the material is crucial in terms of geometry control and material processing aspects. The effect of increased water content on the layer geometry can be recognized in figure 11 and figure 12. Material BM_20 encompasses 52% clay, 38% sand and 20% water in weight, material BM_30 on the other hand is composed of 52% clay, 48% sand, and 30% water.

The study is conducted with a NV of 4000 mm/min and varying VAF from 20 - 45 m³/h, with figure 11 and figure 12 showing the mean value of a number of four tests. The range of LW obtained is 128 - 134 mm for material BM_20 and 172 - 175 mm for material BM_30 as well as a LH of 22 - 25 mm for material BM_20 and 30 - 33 mm for material BM_30. The results represent an equal increase of LH and LW of 30% comparing ND of 150 mm. The LW increases with increased humidity and increased ND, the LH increases with increased moisture content and decreases with increased ND.

Additional fiber reinforcement

Integration of fibers as reinforcement is beneficial for multiple reasons. Depending on the fiber type, it can result in increased compressibility, fracture energy, and ductility [23] of earthen materials. Due to their high moisture regain, low energy demand and good recycling properties, the use of natural,

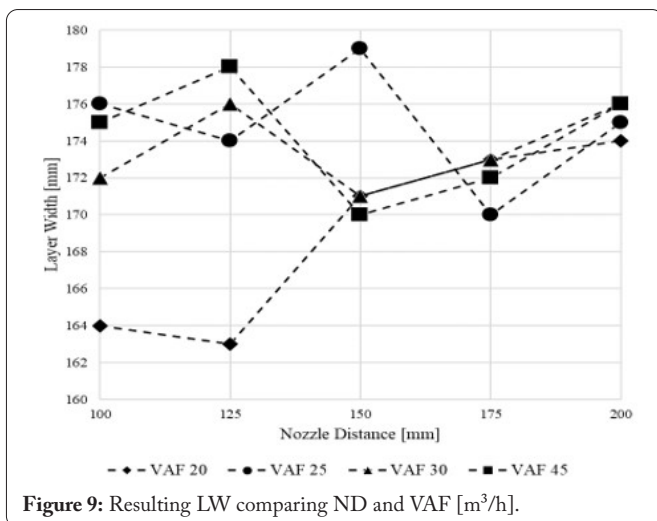


Figure 9: Resulting LW comparing ND and VAF [m³/h].

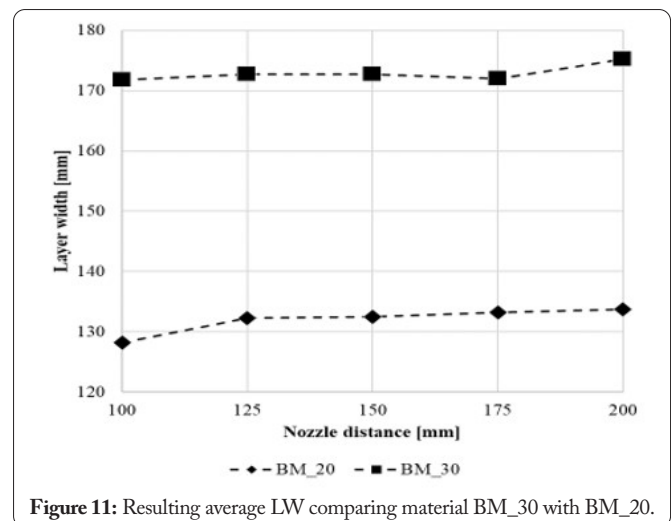


Figure 11: Resulting average LW comparing material BM_30 with BM_20.

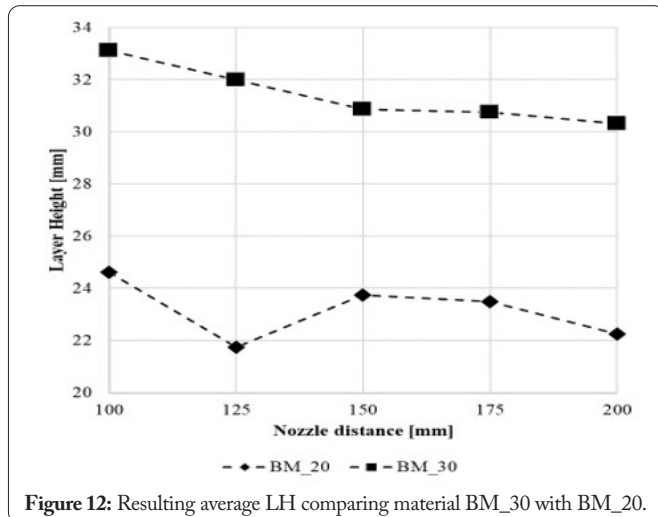


Figure 12: Resulting average LH comparing material BM_30 with BM_20.

organic fibers in earthen construction has been a valid material combination for thousands of years.

Natural fibers are able to speed up the drying process of the earthen material, especially within the first hour of contact, due to the fiber’s moisture regain [24]. This behavior can be seen as beneficial for developing the green strength of the earthen materials right after deposition in additive manufacturing. Moreover, shrinkage can be substantially decreased when using fibers [25], Kouta et al. compared fibers with 12-, 24-, and 50-mm length and concluded that especially long fibers allow for better stress transfer within the material and reduction of stress concentration along micro cracks leading to reduced shrinkage compared to short fibers [23]. On another study, Ferretti et al. investigated the development of stiffness of a printable earthen material comparing two soil-lime mixtures, one with added unaltered rice husk, the other with added shredded rice husk. The study showed that the addition of shredded rice husk leads to higher stiffness due to greater contact surface between the soil/lime mixture while the unaltered rice husk leads to a reaction between the silica contained in the husk and the lime, forming chemical bonds [26].

However, mixing and pumping soil/fiber mixtures is challenging, especially when using longer fibers with a length higher than 30 mm. These tend to accumulate, leading to blockage and inhomogeneous material. In this context, an experimental set up was mounted at DBFL, consisting of a fiber-chopping-gun with a continuous fiber feeding system and a spray nozzle that allows the intermixing of fibers in the material jet after leaving the nozzle (post-nozzle-mixing) (Figure 13 and figure 14).

The fiber chopper used is usually applied for the production of GFRC: glass fiber roving is drawn in over a roller and pressed onto a sharp blade, breaking the fiber. The broken fiber is then sprayed from a spray nozzle by means of air flow. The amount of fiber sprayed is determined by the feed speed of the cutting motor, the speed at which the fibers are sprayed is determined separately by the air flow rate.

Important process parameters here are the alignment of the fiber chopper and the spray nozzle relative to each other,



Figure 13: Experimental test setup with fiber chopper pointing at material jet for post-nozzle intermixing of long fibers.

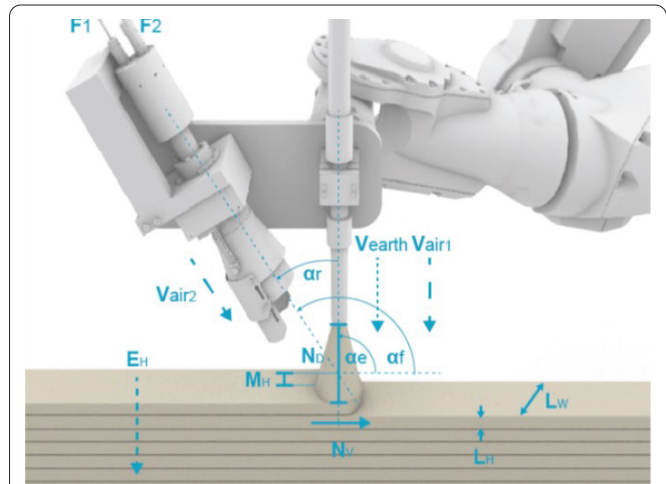


Figure 14: SEAM parameters: nozzle distance (ND) and velocity (NV), layer width (LW), layer height (LH), and earth hardening rate (EH); volume earth (V_{earth}), volume air (V_{air1} and 2), fiber types F1 and F2; spray angle earth (a_e), fibers (a_f), relative earth-fiber angle (a_r), and mixing height (MH).

to ensure mixing of the soil material with the fibers. Here, the air flow rate with which the fibers and the soil material are sprayed, as well as the material quantities, play a decisive role for the homogeneity of the resulting material.

First process-tests showed the method to be feasible. Sprayed fibers and earthen material intermixed in the space between the nozzle and the strand before hitting the target position. It should be noted that a significant portion of the fibers were sprayed through the material-jet and past the sides, so that fibers landed at the interface between subsequent layers. In order to prevent weakening of the interlayer bond through excessive fiber spraying and ensure homogeneous material composition in the strand, precise alignment of the fiber chopper and the spray gun are crucial.

As already described, the use of natural, organic fibers is advantageous for several reasons. Wool fibers have the highest moisture recovery properties of 17% of dead weight, but low tensile strengths of around 0.2 GPa. Jute, flax, and hemp fibers can absorb between 12 and 14% of their own weight in moisture and have tensile strengths between 0.5 GPa (jute) and 0.8 GPa (flax). These considerations present fibers as an interesting compound substance when working with additive manufacturing techniques and clay materials [24].

Summary, Conclusion, and Future Work

In this experimental study, a novel robotic manufacturing process called SEAM was used for the first time. Additionally, tests were conducted on the spraying of long fibers supplementary to the earthen material, so that both materials intermix in the space between the nozzle outlet and the strand. This technique potentially leads to the integration of long, usually non-pumpable fibers in the material mix at the nozzle. Another possible benefit is the drying effect caused by the fiber's ability to regain moisture, especially within 60 minutes after the first contact. This is potentially beneficial for early green strength development of the earthen material after spraying.

In another study, the influence of basic process parameters such as NZ, volume-airstream, and ND on the layer geometry were measured and compared. The study showed that there is a direct influence of the NV and the ND on the LW and LH, which can be described as follows:

- The higher the NV, the lower the LH and LW.
- The higher the ND, the higher the LW and the lower the LH.
- A reduction of the NV has a stronger effect on the LH than on the LW (with a reduction of the NV by 50%, an increase of the LH by 53% and an increase of the NW by 30% was measured).
- The increase in ND tends to have a greater effect on the increase in LW than on the decrease in LH (an increase from 100 to 200 mm causes a 12% increase in LW and a 6% decrease in LH at a NV of 4800 mm/min).
- No direct influence of the VAF on the layer geometry.
- Higher material moisture content leads to increased LW and LH due to increased pumpability.

These findings are principally in line with the results of Dressler et al. [17], who measured the influence of process parameters on the layer geometry in the SC3DP process [27].

Regarding the fabrication of large structures, SEAM presents intriguing possibilities. This technique could offer advantages such as reduced drying times for clay-based additively manufactured structures by leveraging the water absorption capacity of fibers. Additionally, it could potentially enhance construction speed without the necessity of integrating chemical additives for stabilization or liquification, thanks to the positive influence of fiber water absorption. However, it is important to emphasize that these potential effects require rigorous investigation. Consequently, these outcomes constitute the research questions that will be addressed in upcoming research activities at the ITE at TU Braunschweig. Therefore, several studies focusing on the influence on the material properties of different fiber-earth mixtures, fiber length and fiber distribution, as well as investigations on the influence of natural fibers on the development of early green strength are presently being carried out at TU Braunschweig. The controlled cutting of rovings of natural fibers, as well as the homogeneous intermixing of the fibers with the sprayed earthen material, will be further investigated in future planned studies at TU Braunschweig.

Acknowledgements

The experimental work and material research was conducted with the support of the laboratory teams at ITE at TU Braunschweig as well as the Department of Civil and Environmental Engineering (DICEA) of University of Florence. Thanks to the staff members at both institutions for their support and encouragement throughout this process.

Conflict of Interest

None.

References

1. Dubor A, Izard JB, Cabay E, Sollazzo A, Markopoulou A, et al. 2019. On-site Robotics for Sustainable Construction. In Willmann J, Block P, Hutter M, Byrne K, Schork T (eds) *Robotic Fabrication in Architecture, Art and Design* 2018. Springer, Cham, pp 390-401.
2. Goma M, Jabi W, Soebarto V, Xie YM. 2022. Digital manufacturing for earth construction: a critical review. *J Clean Prod* 338: 130630. <https://doi.org/10.1016/j.jclepro.2022.130630>
3. Schweiker M, Endres E, Gosslar J, Hack N, Hildebrand L, et al. 2021. Ten questions concerning the potential of digital production and new technologies for contemporary earthen constructions. *Build Environ* 206: 108240. <https://doi.org/10.1016/j.buildenv.2021.108240>
4. Bock T. 2008. Construction Automation and Robotics. In Balaguer C, Abderrahim M (eds) *Robotics and Automation in Construction*. IntechOpen.
5. 2018 Global Status Report. Global Alliance for Building and Construction. [<https://www.iea.org/reports/2018-global-status-report>] [Accessed September 27, 2023]
6. Easton D. 2012. Pneumatically Impacted Stabilized Earth (PISE) Construction Techniques. In Hall MR, Lindsay R, Krayenhoff M (eds) *Modern Earth Buildings*. Woodhead Publishing, pp. 385-400.
7. Readle D, Coghlan S, Smith JC, Corbin A, Augarde CE. 2016. Fibre reinforcement in earthen construction materials. *Proc Inst Civ Eng Constr Mater* 169(5): 252-260. <https://doi.org/10.1680/jcoma.15.00039>
8. Ashour T, Wieland H, Georg H, Bockisch FJ, Wu W. 2010. The influ-

- ence of natural reinforcement fibres on insulation values of earth plaster for straw bale buildings. *Mater Des* 31(10): 4676-4685. <https://doi.org/10.1016/j.matdes.2010.05.026>
9. Koutous A, Hilali E. 2021. Reinforcing rammed earth with plant fibres: a case study. *Case Stud Constr Mater* 14: e00514. <https://doi.org/10.1016/j.cscm.2021.e00514>
 10. Millogo Y, Morel JC, Aubert JE, Ghavami K. 2014. Experimental analysis of Pressed Adobe Blocks reinforced with *Hibiscus cannabinus* fibers. *Constr Build Mater* 52: 71-78. <https://doi.org/10.1016/j.conbuildmat.2013.10.094>
 11. Watson L, McCabe K. 2011. La técnica constructiva del cob. Pasado, presente y futuro. *Inf Constr* 63(523): 59-70. <https://doi.org/10.3989/ic.10.018>
 12. Hamard E, Cazacliu B, Razakamanantsoa A, Morel JC. 2016. Cob, a vernacular earth construction process in the context of modern sustainable building. *Build Environ* 106: 103-119. <https://doi.org/10.1016/j.buildenv.2016.06.009>
 13. IAAC and WASP: New 3D Printing Strategies Towards the Realisation of Load-bearing Earthen Structures. [<https://iaac.net/iaac-wasp-new-3d-printing-strategies-towards-realisation-load-bearing-earthen-structures/>] [Accessed September 27, 2023]
 14. TECLA Technology and Clay 3D Printed House / Mario Cucinella Architects. [<https://www.archdaily.com/960714/tecla-technology-and-clay-3d-printed-house-mario-cucinella-architects>] [Accessed September 27, 2023]
 15. Kloft H, Lowke D, Hack N. 2019. Shotcrete 3D Printing (SC3DP)-an innovative and efficient technology for 3D printing of large-scale concrete components. *Drymix Mortar Yearbook 3D Special*; Drymix. info: München, Germany, 38-43.
 16. Hack N, Kloft H. 2020. Shotcrete 3D Printing Technology for the Fabrication of Slender Fully Reinforced Freeform Concrete Elements with High Surface Quality: A Real-scale Demonstrator. In Bos F, Lucas S, Wolfs R, Salet T (eds) *Second RILEM International Conference on Concrete and Digital Fabrication*, RILEM Bookseries. Springer, Cham, pp 1128-1137.
 17. Dressler I, Freund N, Lowke D. 2020. The effect of accelerator dosage on fresh concrete properties and on interlayer strength in shotcrete 3D printing. *Materials* 13(2): 374. <https://doi.org/10.3390/ma13020374>
 18. Van Der Putten J, De Schutter G, Van Tittelboom K. 2018. The Effect of Print Parameters on the (Micro) Structure of 3D Printed Cementitious Materials. In Wangler T, Flatt R (eds) *First RILEM International Conference on Concrete and Digital Fabrication*, RILEM Bookseries. Springer, Cham, pp 234-244.
 19. Marchment T, Sanjayan JG, Nematollahi B, Xia M. 2019. Interlayer Strength of 3D Printed Concrete: Influencing Factors and Method of Enhancing. In Sanjayan JG, Nazari A, Nematollahi B (eds) *3D Concrete Printing Technology*. Butterworth-Heinemann, pp 241-264.
 20. Le TT, Austin SA, Lim S, Buswell RA, Law R, et al. 2012. Hardened properties of high-performance printing concrete. *Cem Concr Res* 42(3): 558-566. <https://doi.org/10.1016/j.cemconres.2011.12.003>
 21. Future is Made of Clay. Building Ecologically. Of course with Clay. [<https://www.conluto.de/>] [Accessed September 27, 2023]
 22. Heidarneszhad F, Zhang Q. 2022. Shotcrete based 3D concrete printing: state of art, challenges, and opportunities. *Constr Build Mater* 323: 126545. <https://doi.org/10.1016/j.conbuildmat.2022.126545>
 23. Kouta N, Saliba J, Saiyouri N. 2020. Effect of flax fibers on early age shrinkage and cracking of earth concrete. *Constr Build Mater* 254: 119315. <https://doi.org/10.1016/j.conbuildmat.2020.119315>
 24. Beckman IP, Lozano C, Freeman E, Riveros G. 2021. Fiber selection for reinforced additive manufacturing. *Polymers* 13(14): 2231. <https://doi.org/10.3390/polym13142231>
 25. Fanguero R, Rana S. 2016. *Natural Fibres: Advances in Science and Technology Towards Industrial Applications*. Springer, Dordrecht.
 26. Ferretti E, Moretti M, Chiusoli A, Naldoni L, De Fabritiis F, et al. 2022. Rice-husk shredding as a means of increasing the long-term mechanical properties of earthen mixtures for 3D printing. *Materials* 15(3): 743. <https://doi.org/10.3390/ma15030743>
 27. Dressler I, Freund N, Lowke D. 2020. Control of Strand Properties Produced with Shotcrete 3D Printing by Accelerator Dosage and Process Parameters. In Bos F, Lucas S, Wolfs R, Salet T (eds) *Second RILEM International Conference on Concrete and Digital Fabrication*, RILEM Bookseries. Springer, Cham, pp 42-52.